Physical Communication 35 (2019) 100680

Contents lists available at ScienceDirect

Physical Communication

journal homepage: www.elsevier.com/locate/phycom

Full length article

Fading-aligned OFDM with index modulation for mMTC services

Ebubekir Memisoglu [a,*], Ertugrul Basar [b], Huseyin Arslan [c,d]

[a] Faculty of Electrical and Electronics Engineering, Istanbul Technical University, Maslak 34469, Istanbul, Turkey
[b] Communications Research and Innovation Laboratory (CoreLab), Department of Electrical and Electronics Engineering, Koç University, Sariyer 34450, Istanbul, Turkey
[c] Department of Electrical and Electronics Engineering, Istanbul Medipol University, 34810 Istanbul, Turkey
[d] Department of Electrical Engineering, University of South Florida, 33620 Tampa, USA

ARTICLE INFO

Article history:
Received 29 September 2018
Received in revised form 16 January 2019
Accepted 13 March 2019
Available online 29 March 2019

Keywords:
Circular shifting
Energy efficiency
Fading alignment
mMTC
OFDM-IM
Spectral efficiency

ABSTRACT

5th generation (5G) of wireless networking is coming with diverse use cases, such as enhanced-Mobile BroadBand (eMBB), Ultra Reliable and Low Latency Communications (URLLC), and massive Machine Type Communications (mMTC). As a result, 5G wireless networks require flexible physical layer solutions through new radio access technologies (RATs). At this point, orthogonal frequency division multiplexing with index modulation (OFDM-IM) appears a flexible solution to satisfy the diverse user demands. Considering the strict requirements of mMTC services, such as low throughput, low power consumption, and low cost design, we propose fading-aligned OFDM-IM for more spectrum- and energy-efficient communication. In the proposed method, inactive subcarriers in OFDM-IM are cleverly utilized to avoid deep fading sub-channels, because the deep fading of the active subcarriers decreases bit error rate (BER) performance significantly. Computer simulation results demonstrate that more than 10 dB gain is obtained for a reference BER value of 10^{-4} at the same spectral efficiency with conventional OFDM. Moreover, the proposed method is compared with convolutional coded (CC) OFDM at the same spectral efficiency, and it is shown that the proposed scheme performs better in terms of BER performance. Furthermore, theoretical error performance of the proposed method is investigated to support our computer simulations.

1. Introduction

In the context of application rich and aware communication networks, 5G New Radio (NR) requires flexible radio access technologies (RATs) to support the diverse requirements of wide range of applications [1] and [2]. In 5G wireless networking, there are mainly three service types: enhanced-Mobile BroadBand (eMBB), Ultra Reliable and Low Latency Communications (URLLC), and massive Machine Type Communications (mMTC). Orthogonal frequency division multiplexing (OFDM) with multi-numerologies has been selected as the core waveform of 5G to meet the requirements of different services [3]. Therefore, the technologies that will be developed for different services in 5G have to be flexible and suitable with the OFDM waveform. Within this perspective, for RATs beyond 5G, a framework for flexible waveform, numerology, and frame design strategies is investigated to shed light on the scope of next-generation communication systems [4].

In mMTC services, the following requirements need to be satisfied [5]:

(i) Low throughput
(ii) Low power
(iii) Low cost
(iv) Massive connectivity
(v) Wider coverage.

Achieving only a low throughput is not a major problem; however, it has some limitations based on the requirements of low power consumption and low cost. Furthermore, the use of a single antenna, narrow bandwidth operation, and new power saving modes are needed to achieve low power consumption and low-cost requirements. From the spectrum utilization perspective, the vision of billions of interconnected devices will require more efficient solutions to share the available spectrum for the massive connectivity. Additionally, the improvements in power consumption, message repetition, and relaxed performance requirements can be used for the wider coverage. Therefore, the development of spatial diversity and frequency diversity methods is very challenging to improve the bit error rate (BER) performance due to the design choices made for mMTC services.

* Corresponding author.
E-mail addresses: memisoglu17@itu.edu.tr (E. Memisoglu), ebasar@ku.edu.tr (E. Basar), huseyinarslan@medipol.edu.tr (H. Arslan).

https://doi.org/10.1016/j.phycom.2019.03.008
1874-4907/

In the literature, the knowledge of the channel state information (CSI) in the transmitter is utilized for different purposes, such as adaptive modulation and coding [6], antenna selection in spatial modulation (SM) systems [7], joint peak-to-average power ratio (PAPR) reduction and out-of-band emission (OOBE) suppression [8], precoder design for beamforming and multiple-input multiple-output (MIMO) [9], and physical (PHY) and medium access control (MAC) layers security [10] and [11]. Adaptive modulation and coding maximizes the spectral efficiency by varying data rate, code rate, transmit power, and instantaneous BER. Antenna selection depending on different selection techniques achieves a significant gain in signal-to-noise ratio (SNR) by exploiting spatial diversity in SM systems. In order to solve two critical disadvantages of the OFDM waveform, which are high PAPR and high OOBE, a number of special alignment processes are employed. In a MIMO system, beamforming is deployed to achieve a better system performance. For secure communication, a number of techniques for PHY and MAC layers are developed with minimal capacity losses.

As an enhancement modulation technique to OFDM waveform with additional modulation flexibility, OFDM-IM has been proposed for spectrum- and energy-efficient wireless communication systems inspired by the concept of SM [12] and [13]. It is also suitable with multi-numerology OFDM. In OFDM-IM, unlike conventional OFDM, both active and inactive subcarriers exist in the OFDM symbol for the transmission of data symbols and IM bits, respectively. Thus, the IM concept brings some attractive advantages for classical OFDM in some conditions, such as better BER performance, robustness to inter-carrier interference (ICI), flexibility to different channel conditions and system requirements, and well-suitability to vehicular, machine-to-machine (M2M), and device-to-device (D2D) communication systems [14]. However, the knowledge of the CSI in the transmitter is not utilized well for different purposes in OFDM-IM schemes. Recently, in order to utilize the CSI for dual-mode OFDM-IM [15], adaptive dual mode IM technique has been proposed to increase the spectral efficiency further compared to plain OFDM-IM [16]. Also, in the work of [17], OFDM with subcarrier index modulation (OFDM-SIS) is proposed inspiring by the IM concept to improve the security and the reliability of URLLC services using joint optimal subcarrier index selection and adaptive interleaving techniques.

In spite of its attractive advantages, OFDM-IM has a limited spectral efficiency for strong SNR values where higher order modulations are employed. Consequently, it cannot meet eMBB service requirements such as high throughput. However, the recent works of [18] and [19] showed that multiple-mode OFDM-IM achieves a high spectral efficiency with a better BER performance at high SNR values. In this scheme, multiple distinguishable signal constellation are employed using low complexity detectors. As a result, the IM concept can suit to the diverse use cases with different techniques. Moreover, it has a potential to be used on various areas for different purposes [14]. It has been also shown that OFDM-IM is well-suited to MIMO systems [20] and [21].

The existence of inactive subcarriers in OFDM-IM can be utilized for more spectrum- and energy-efficient communication. In the frequency selective channel, the deep fading sub-channels do not affect the inactive subcarriers, because they convey information in the space domain. Therefore, in this paper, we propose a fading alignment method to avoid deep fading sub-channel usage for OFDM-IM. The alignment is performed by a circular shift depending on the CSI at the transmitter as seen from Fig. 1. However, our method is not capable of avoiding all deep fading sub-channels that are determined according to a threshold value. The reason of this phenomenon can be explained by the fact that the success of avoiding deep fading sub-channels depends on the activation ratio, channel conditions, and amount of the sub-channels to be avoided. Furthermore, a mapping technique as in [22] and coordinate interleaving method [23] can be used to improve performance of the proposed method. Although not avoiding all deep fading sub-channels, our proposed method provides a significant gain in BER performance without any data rate reduction. At the receiver, a reverse alignment procedure is employed to detect the transmitted information correctly. Due to the requirements such as low throughput and low power consumption, OFDM-IM appears an attractive modulation technique for mMTC services. Here, our main contribution is the utilization of inactive subcarriers for deep fading avoidance in OFDM-IM to improve the spectral and energy efficiency for critical mMTC applications.

The remainder of this paper is organized as follows. In Section 2, the system model is described for the proposed method. The transceiver architecture of the proposed method is explained in Section 3. The theoretical error performance of the proposed method is investigated in Section 4. Then, computer simulation results are demonstrated in Section 5. Finally, the paper is concluded in Section 6.

Notation: Bold, lower-case and capital letters denote vectors and matrices, respectively. The transposition and Hermitian transposition are denoted by $(.)^T$ and $(.)^H$, respectively. $\mathbb{S}$ indicates the set of constellation symbols. $\mathbf{I}_N$ is the identity matrix with dimensions of $N \times N$. $\mathcal{CN}(0, \sigma^2)$ denotes the circularly symmetric complex Gaussian distribution with variance σ^2. $\mathbb{C}$ denotes the ring of complex numbers. The expected value, the floor function, and the tail probability of standard Gaussian distribution are denoted by $E[.]$, $\lfloor . \rfloor$ and $Q(.)$, respectively. $C(n, k)$ denotes the binomial coefficient.

2. System model

We consider a single-input single-output (SISO) OFDM-IM system architecture transmitting over a slowly varying Rayleigh multipath fading channel as shown in Fig. 1. This system model suits to mMTC service features, such as single antenna usage for low cost implementation, low mobility, and frequency selectivity. It is assumed that the CSI is perfectly known at the transmitter and the receiver, which is a reasonable assumption for time division duplexing operation. Furthermore, a few number of bits are transmitted correctly over a secure link to convey the shifting information to the receiver, where this information is used at the receiver for the proposed method and will be explained in detail later. The CSI does not need to be estimated for each transmission time by the receiver, because it is assumed that the channel varies slowly.

Here, a total of m bits entering the system are divided into two groups: The first group of bits determine the active subcarriers' indices for the subblocks of an OFDM-IM symbol according to a given look-up table, while the remaining group of bits are employed to determine M-ary constellation symbols for the activated subcarriers. After IM process is completed, the OFDM-IM block is represented as

$$\mathbf{x}_F = [x(1)\, x(2)\, \ldots\, x(N)]^T \tag{1}$$

where $x(j) \in \mathbb{S}$ for the activated subcarriers, otherwise $x(j) = 0$, $j = 1, 2, \ldots, N$ in the frequency domain (FD). In order to make all subcarriers in a subblock uncorrelated with each other, a $G \times N$ block interleaver is employed where G is the total number of the subblocks in an OFDM-IM symbol as in [24]. After obtaining the interleaved block $\tilde{\mathbf{x}}_F$, a circular shifting process is employed, where $\tilde{\mathbf{s}}$ is the circularly shifted version of $\tilde{\mathbf{x}}_F$. Here, the amount of circular shift is determined by the CSI and as mentioned previously, conveyed to the receiver through a secure link. In Section 3, this technique will be explained in more detail.

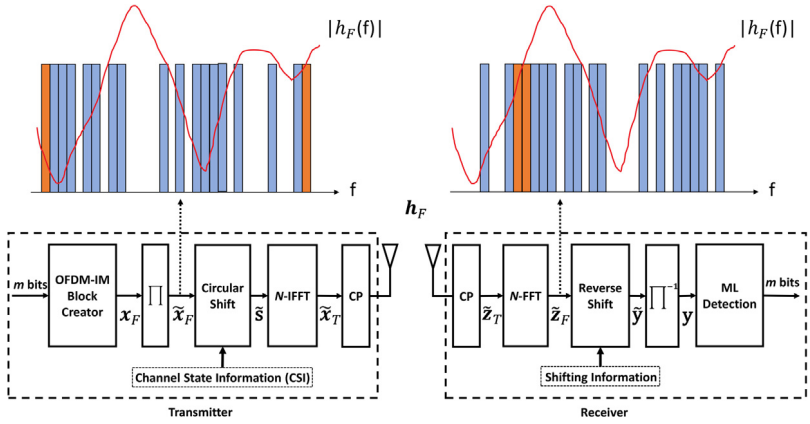

Fig. 1. Block diagram of the proposed method. The blue and orange rectangles show active subcarriers in an OFDM-IM symbol. The orange rectangles are used to demonstrate the circular shift of the subcarriers.

After the FD processes, the time domain (TD) OFDM-IM signal is obtained by taking the inverse fast Fourier transform (IFFT) of $\tilde{\mathbf{s}}$:

$$\tilde{\mathbf{x}}_T = \frac{N}{\sqrt{K}}\text{IFFT}\{\tilde{\mathbf{s}}\} = \frac{1}{\sqrt{K}}\mathbf{F}_N^H\tilde{\mathbf{s}} \tag{2}$$

where $\mathbf{F}_N$ is the discrete Fourier transform (DFT) matrix with $\mathbf{F}_N^H\mathbf{F}_N = N\mathbf{I}_N$. $(N/\sqrt{K})$ is the normalization factor to have the same average transmission energy with conventional OFDM, where K is the total number of active subcarriers in an OFDM-IM symbol. Then, a cyclic prefix (CP) of length C_p is added to avoid inter-symbol interference (ISI) in a multipath fading channel. Before transmitting the TD signal $\tilde{\mathbf{x}}_T$ over a frequency selective fading channel, parallel to serial and digital-to-analog conversions are performed.

After removing the CP part from the received signal, the FFT operation is deployed for $\tilde{\mathbf{z}}_T$ to obtain the FD signal $\tilde{\mathbf{z}}_F$ at the receiver side. Then, a circular reverse shifting operation is performed based on the shifting information to obtain $\tilde{\mathbf{y}}$. Before the maximum likelihood (ML) detection, an $N \times G$ block de-interleaver is considered to obtain $\mathbf{y}$. Next, $\mathbf{y}$ is expressed in the scalar form as

$$y(j) = x(j)\hat{h}_F(j) + w_F(j), \quad j = 1, 2, \ldots, N \tag{3}$$

where $w_F(j) \sim \mathcal{CN}(0, N_{0,F})$ is the additive white Gaussian noise sample and $\hat{h}_F(j) \sim \mathcal{CN}(0, 1)$ is the channel fading coefficient in the FD. Here, $N_{0,F} = (K/N)N_{0,T}$ is the noise variance in FD, $\hat{\mathbf{h}}_F \in \mathbb{C}^{N\times 1}$ is the $N \times G$ deinterleaved and circular reverse shifted version of $\mathbf{h}_F$ based on the shifting information, and $\mathbf{h}_F \in \mathbb{C}^{N\times 1}$ is the FD representation of the channel impulse response (CIR) $\mathbf{h}_T = [h_T(1)\ h_T(2)\ \ldots\ h_T(L)]^T$, where $h_T(j)$, $j = 1, \ldots, L$ are circularly symmetric complex Gaussian random variables with the $\mathcal{CN}(0, 1/L)$ distribution. Finally, the SNR is calculated as $E_b/N_{0,T}$, where E_b is the average energy per bit.

At the last step, ML detection is used to detect the active subcarriers and the corresponding data symbols optimally as in [12]; however, greedy detection (GD) [25] should be employed for lower complexity considering mMTC requirements, especially in the case of large IM subblocks. After the detection, the corresponding bits are obtained.

3. Proposed method

In the OFDM system, consecutive subcarriers may fade deeply in the frequency-selective channel. In order to cope with the errors occurred by this reason, coded OFDM (COFDM) has been chosen for most of the practical OFDM-based systems. For this purpose, forward error correction (FEC) codes, such as convolutional codes, turbo codes, low density parity check (LDPC) codes, and so on, are employed. However, FEC codes cannot completely remove the effects of deep fading. Also, interleaving is often employed to improve the performance gain of the COFDM system.

As being differently from conventional OFDM, a selected number of subcarriers are not used for the signal transmission due to IM in OFDM-IM. These unutilized subcarriers still carry information in the space domain. Thus, they are not directly affected by deep fading in the frequency selective channel. Due to this reason, we propose a channel-based fading alignment procedure for the OFDM-IM subcarriers using the circular shifting operation to avoid deep fading sub-channels. Before the circular shifting, block interleaving is employed to make the channel uncorrelated for subblocks and convert the inactive subcarrier distribution into random.

Algorithm 1 Circular shifting for fading alignment at the transmitter

```
procedure FadeAlign( u, v, r)
    u ← OFDM-IM block
    v ← CFR
    r ← threshold value
    for i = 1 → N do
        if |h(i)|> r then
            h(i) ← r
        end if
    end for
    max ← 0
    for i = 1 → (N − 1) do
        s(i) ← |v^T u|
        if s(i) > max then
            max ← s(i)
            shift ← i − 1
            s ← u
        end if
        u ← [u(N) u(1) u(2) ... u(N − 1)]
    end for
    return s & shift
end procedure
```

Algorithms 1 and 2 are employed for the proposed method in the transmitter and the receiver, respectively. In Algorithm 1, the interleaved OFDM-IM block in FD, the channel frequency response (CFR), and the threshold value that determines the deep fading sub-channels are denoted by $\mathbf{u}$, $\mathbf{v}$, and r, respectively. Here, N stands for the size of the OFDM-IM block. The CFR vector is reformed based on the threshold value of r. If the absolute value of the channel coefficient is higher than r, this coefficient is replaced by the r value to consider only the deep fading sub-channels

in the circular shifting operation. So, the limited resource of the inactive subcarriers is just utilized to avoid the deep fading sub-channels. Then, the circular shifting is performed to find the best alignment. If the absolute value of $\mathbf{v}^T\mathbf{u}$ is maximum, deep fading sub-channels are avoided and $\mathbf{u}$ is shifted circularly for the best alignment to avoid deep fading sub-channels. This procedure avoids the deep fading sub-channels as much as the system capability allows depending on the activation ratio, mapping scheme, shifting process and r. After finding the best alignment with circular shifting, the algorithm returns the shifted version of $\mathbf{u}$ and the amount of shifting information as $\mathbf{s}$ and *shift*, respectively. The *shift* information is forwarded correctly to the receiver. For this, FEC codes can be used for the shifting information, or a pattern that is inserted into OFDM-IM block to detect the amount of shifting in the receiver can even be used without sending the shifting information. We would like to note that these issues are out of scope of this work.

Algorithm 2 Reverse shifting at the receiver

```
procedure ReverseAlign( z, v, l)
    z ← received signal
    v ← CFR
    l ← amount of shifting
    y ← [z(l+1) z(l+2)...z(N) z(1) z(2)...z(l)]
    v ← [v(l+1) v(l+2)...v(N) v(1) v(2)...v(l)]
    return y & v
end procedure
```

In Algorithm 2, the received signal in FD, the CFR, the *shift* information that represents the amount of shifting are taken as $\mathbf{z}$, $\mathbf{v}$, and l, respectively. At the receiver, this algorithm returns to the initial stage before alignment by using l information. Also, same shifting process is applied to $\mathbf{v}$ for the ML detection in the receiver.

For the computational complexity of the proposed method, only the number of multiplications is considered. At the transmitter, $N \times (N-1)$ multiplications are performed to find the best alignment. Furthermore, this computational complexity can be decreased easily; however, these algorithms have been developed heuristically without investigating improvements. Because the absolute channel coefficient values that are larger than r do not have importance, these multiplications are unnecessary. Also, the circular shifting can be done with more than an subcarrier for each loop in order to decrease the complexity. On the other hand, there is no multiplication operation at the receiver for reverse alignment, only one circular shift is sufficient. Therefore, the computational complexity does not increase at the receiver.

4. Performance analysis

In this section, we provide an approximate error performance analysis for the proposed fading-aligned OFDM-IM scheme to gain further insights about its improved performance. In order to evaluate the performance of the proposed method, the indices of the active subcarriers and data symbols are detected separately with employing GD at the receiver to make the theoretical error probability derivations feasible and to provide a lower-bound on the achievable error rate. Here, the gain comes from the avoidance of deep fading sub-channels, and the fading alignment for this purpose changes the envelope distribution of the effective sub-channels at the receiver. As seen from Fig. 2, the envelope distribution of the proposed method starts from the r value, where $r \geq 0$ denotes the threshold value to determine the deep fading sub-channels. Here, $\zeta = k/n$ represents the activation ratio for IM, where k is the number of active subcarriers and n is the number of available subcarriers in an IM subblock. However, the proposed method cannot guarantee the avoidance of all deep fading sub-channels. Moreover, other various parameters affect this distribution as well. Therefore, the distribution is approximated as a partial Rayleigh distribution to find the theoretical BER performance,

$$f(\alpha) \approx \frac{\alpha}{\sigma^2} e^{-\alpha^2/\left(2\sigma^2\right)}, \quad \alpha \geq r, \tag{4}$$

where $\alpha = |h_F(\beta)|$, $\beta \in \mathbb{I}$ with $\mathbb{I}$ being the set of active subcarrier indices, and σ is the scaling parameter of the Rayleigh distribution.

At the receiver, the effective instantaneous SNR and the average SNR for each subcarrier in FD can be defined as

$$\gamma = \frac{|\alpha|^2 \varphi E_b}{N_{0,F}} \tag{5}$$

$$\bar{\gamma} = E\{\gamma\} = \frac{a\varphi E_b}{N_{0,F}} \approx \frac{\varphi E_b}{N_{0,F}} \tag{6}$$

where $\varphi = n/k$ and $a = E[|\alpha|^2]$ equals approximately to unity when r is a small value such as 0.1. And, the probability density function of partial chi-square distributed γ is given by

$$p(\gamma) \approx \frac{1}{\bar{\gamma}} \exp\left(-\frac{\gamma}{\bar{\gamma}}\right), \quad \gamma \geq b, \tag{7}$$

where $b = r^2 \varphi E_b / N_{0,F}$.

The approximated average bit error probability P_b of the proposed method can be expressed as in [26]

$$P_b \approx \frac{p_1 P_1 + p_2 P_2}{p_1 + p_2}, \tag{8}$$

where $p_1 = \lfloor \log_2(C(n,k)) \rfloor$, $p_2 = \log_2 M$, P_1, and P_2 respectively denote the number of index bits, the number of symbol bits, the index BER, and the symbol BER. Therefore, we need to find P_1 and P_2 to evaluate the P_b.

Here, P_1 can be approximated as

$$P_1 \approx \mu \bar{P}_I / 2, \tag{9}$$

where $\bar{P}_I$ is the average index error probability and $\mu = 1, 2$ for $n = 2$ and $n > 2$, respectively. In order to derive $\bar{P}_I$ from the index error probability P_I, a simpler version of P_I is used as in [27]

$$P_I \approx \frac{k}{n} \sum_{\beta=1}^{n} \frac{(n-k)}{2} \exp\left(-\frac{\gamma}{2}\right) = k \frac{(n-k)}{2} E\left[-\frac{\gamma}{2}\right], \tag{10}$$

For our proposed method, $\bar{P}_I$ can be calculated approximately as in [28]

$$\bar{P}_I \approx \frac{(n-k)}{2} \int_b^\infty \exp(-\gamma/2) p(\gamma) d\gamma, \quad b \geq 0 \tag{11}$$

$$= \frac{(n-k)}{2} \int_r^\infty \exp(-\alpha^2 \bar{\gamma}/2) 2\alpha \exp(-\alpha^2) d\alpha, \quad r \geq 0 \tag{12}$$

where (12) is obtained from the integration by the substitution of $\gamma = \alpha^2 \bar{\gamma}$.

After obtaining $\bar{P}_I$, P_2 can be expressed as

$$P_2 \leq \frac{\bar{P}_I}{2k} + \frac{\bar{P}_M}{p_2}, \tag{13}$$

where $\bar{P}_M$ represents the average symbol error probability. Since BPSK ($M = 2$) is used for data modulation in computer simulations, $\bar{P}_M$ can be obtained as

$$\bar{P}_M = \frac{1}{2} \int_b^\infty \operatorname{erfc}(\sqrt{\gamma}) p(\gamma) d\gamma, \quad b \geq 0 \tag{14}$$

$$= \int_r^\infty Q\left(\sqrt{2\alpha^2 \bar{\gamma}}\right) 2\alpha \exp(-\alpha^2) d\alpha, \quad r \geq 0 \tag{15}$$

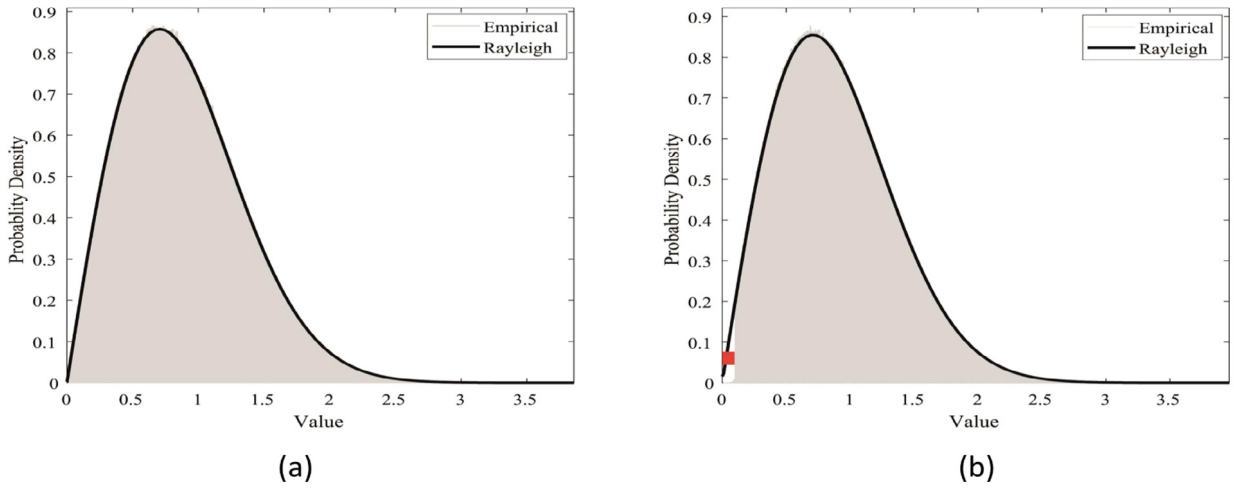

Fig. 2. The envelope distributions of the effective sub-channels for (a) conventional OFDM-IM with $r = 0$ and (b) the proposed method with $r = 0.1$, $\zeta = 1/2$, and $L = 15$. The red rectangle shows the effect of avoidance from deep fading sub-channels.

where (15) is obtained from the integration by the substitution and using the identity

$$Q(x) = \frac{1}{2}\text{erfc}\left(\frac{x}{\sqrt{2}}\right). \tag{16}$$

Finally, to find the approximated P_b, the derived (9) and (13) are inserted into (8).

In Fig. 3, BER performance curves of the proposed method are given for $L = 15$ and compared with conventional OFDM-IM, where we also show approximated theoretical curves and consider index and data symbol errors with GD at the receiver. As seen from Fig. 3, theoretical and simulation results are in agreement. The SNR gain difference between the theoretical and the simulation BER curves for the proposed method is due to the distribution change and the failure of avoiding all deep fading sub-channels. To decrease this difference, more feasible activation ratio ζ and r values can be chosen. It is worth noting that there are other parameters that affect the performance of the deep fading avoidance as mentioned earlier.

Remark. In order to evaluate the performance of the proposed method based on the parameters of r, ζ, and L, Table 1 has been created by generating 10^5 OFDM-IM symbols. Success rate percentages are obtained by dividing the total number of the non-deep fading active subcarriers to the total number of the active subcarriers. Here, non-deep fading active subcarriers are determined according to the r value. If the absolute magnitude of the active subcarrier channel is larger than r, it is determined as a non-deep fading active subcarrier. Otherwise, it is determined as a deep fading active subcarrier. As seen from Table 1, the success rates change for different cases. If r and ζ are small and L is large, the success rate increases. Here, the selection of the r should be determined based on ζ and L values for the better performance. When $r = 0$, the proposed method turns into conventional OFDM-IM. It is also worth noting that the spectral efficiency decreases for the small ζ values. Furthermore, more diverse selective channel provides the better performance.

5. Simulation results

In this section, we provide computer simulation results to show the performance of proposed method under the different conditions. In order to understand the impact of the subcarrier activation ratio in the proposed method, two different activation ratio values $\zeta = 1/2$ and $\zeta = 1/4$ are considered for IM.

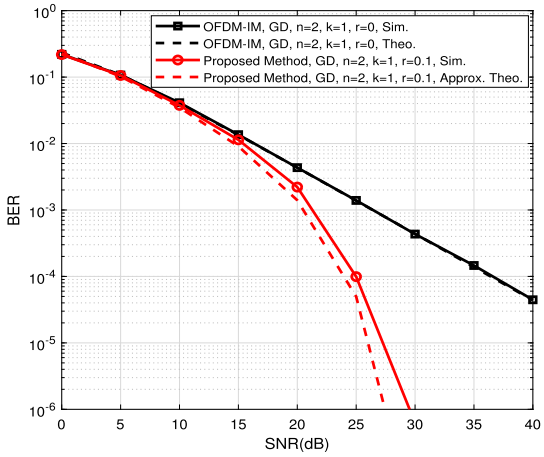

Fig. 3. The theoretical BER performance of the proposed method.

Table 1
Deep fading avoidance success rates for the different r, ζ, and L values.

$L = 2$				$L = 10$			
r	ζ			r	ζ		
	1/2	1/4	1/8		1/2	1/4	1/8
0.1	82.9%	96.7%	99.3%	0.1	97.9%	99.9%	99.9%
0.2	71.2%	91.2%	97.7%	0.2	89.4%	99.0%	99.9%
0.3	65.2%	86.9%	95.7%	0.3	78.7%	95.8%	99.6%

For different channel conditions, the length of channel impulse response (L) is taken as $L = 2$, $L = 10$, and $L = 15$ where the length of C_p is always larger than L for the Rayleigh multi-path fading channel. Unless stated otherwise, the length of L and the activation ratio are taken as $L = 10$ and $\zeta = 1/2$. The symbol block size and C_p length are taken as $N = 128$ and $C_p = 16$ and we adopt BPSK modulation throughout the simulations. Here, it is assumed that an OFDM-IM subblock consists of four subcarriers. Moreover, the spectral efficiency of the proposed method can be increased by using the larger size of an OFDM-IM subblock. However, this is not considered in this paper.

Fig. 4 shows the BER performance of the proposed method for different threshold values (r) in comparison to OFDM-IM and conventional OFDM. We observe that the proposed scheme provides a significant gain in BER without any spectral efficiency

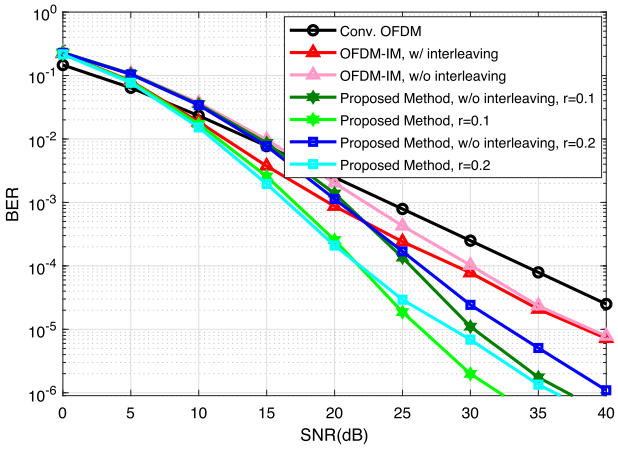

Fig. 4. The BER performance of the proposed method for $\zeta = 1/2$.

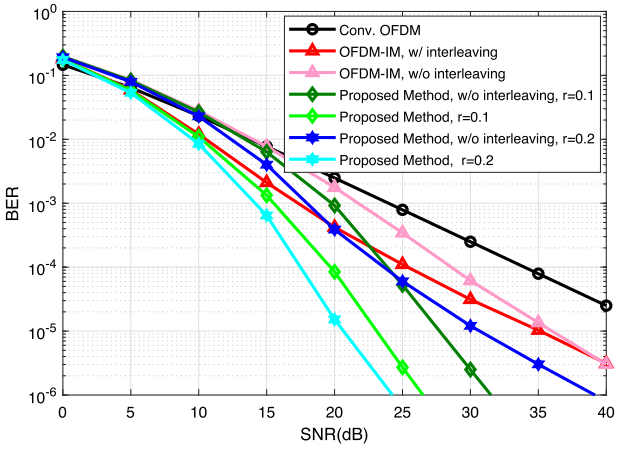

Fig. 5. The BER performance of the proposed method for $\zeta = 1/4$.

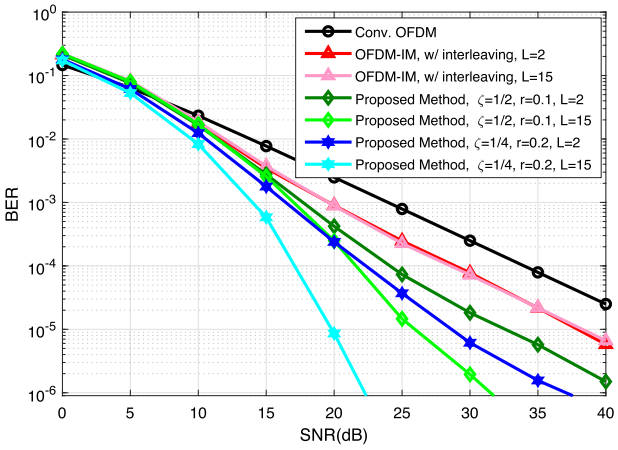

Fig. 6. The BER performance of the proposed method for the different channel conditions.

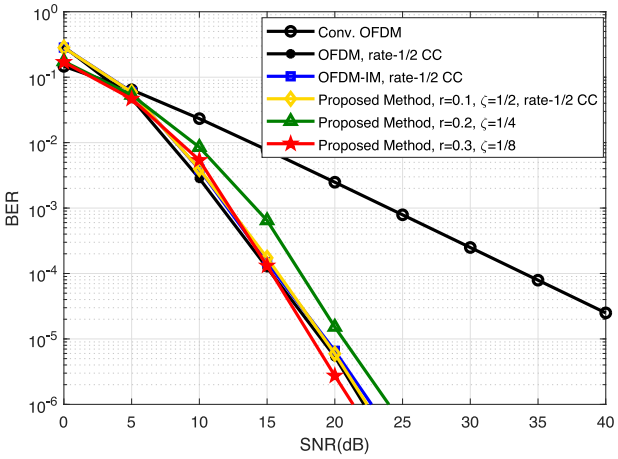

Fig. 7. The BER performance comparison of the proposed method with the convolutional coded (CC) OFDM.

reduction. Here, our system performance depends on interleaving, the r value, the activation ratio, and the channel itself. In the proposed method, interleaving provides approximately 5 dB more gain in the high SNR values unlike OFDM-IM, because it distributes the inactive subcarriers randomly to increase the avoidance success of the fading sub-channels. The cross sections of the lines that have different r values show that r has to be determined independently for each SNR value, however, only one r value is taken by considering high SNR values for simplicity. Thus, the system capability and the SNR value are needed to be considered jointly because of the limited capability to avoid deep fading sub-channels.

In Fig. 5, the impact of a different activation ratio is demonstrated. We demonstrate that if the activation ratio of the active subcarriers decreases, the success of the avoidance increases, so a higher r value can be chosen to ensure a better BER performance. Although the lower activation ratio means controllable reduction at the spectral efficiency, the improvement in BER compared to $\zeta = 1/2$ case is about 8 dB for the reference BER value of 10^{-6}. From the perspective of frequency-selective channel, an increasing number of taps (L) means more frequency selectivity. Due to the better success rate of deep fading avoidance, the proposed method achieves a better performance in more frequency selective channels as seen from Fig. 6. OFDM-IM gives better performance than conventional OFDM in the frequency selective channel, however, as differently from the proposed method, it does not improve the performance in a more frequency selective channel when interleaving is used.

On the other hand, the proposed method is compared with the coded OFDM-IM and OFDM in Fig. 7. For coding, the rate-1/2 convolutional code (CC) is considered [28] without interleaving. For fair comparison, interleaving has to also be used in COFDM, but this comparison is done due to demonstrate that the deep fading channel effects can be solved with the proposed method with the significant BER performance close to the BER performance of CC in COFDM. As seen from this figure, the proposed scheme performs better in BER than the COFDM at the same spectral efficiency where the activation ratio is selected as $\zeta = 1/8$, which is a noticeable result. However, the combination of the proposed method and the CC does not improve the BER performance significantly, because both of them try to avoid fading sub-channels, separately.

6. Conclusion

In this paper, we have proposed a fading alignment technique in OFDM-IM for mMTC services. For this purpose, circular shift and reverse shift operations have been employed at the transmitter and the receiver, respectively. It has been demonstrated that the avoidance of deep fading sub-channels provides a significant gain in BER performance over OFDM-IM and conventional OFDM at the same spectral efficiency in the frequency selective channel. Moreover, for different activation ratios and channel conditions,

the proposed method has been investigated. We have shown by extensive computer simulations that the proposed method performs better in terms of BER performance with a lower activation ratio in a more frequency selective channel. Furthermore, our comparison with the rate-1/2 CC has demonstrated that the proposed method provides a better BER performance at the same spectral efficiency.

For the future work, the proposed alignment technique can be exploited for PAPR reduction and physical-layer security by the addition of artificial noise over the deep fading subcarriers at the transmitter.

References

[1] M. Shafi, et al., 5G: a tutorial overview of standards, trials, challenges, deployment, and practice, IEEE J. Sel. Areas Commun. 35 (6) (2017) 1201–1221.

[2] A.A. Zaidi, et al., Waveform and numerology to support 5G services and requirements, IEEE Commun. Mag. 54 (11) (2016) 90–98.

[3] 3rd Generation Partnership Project (3GPP), NR; Physical channels and modulation, Technical Specification 38.211, ver. 15.1.0, Apr. 2018.

[4] Z.E. Ankarali, B. Peköz, H. Arslan, Flexible radio access beyond 5G: a future projection on waveform, numerology, and frame design principles, IEEE Access 5 (2017) 18295–18309.

[5] C. Bockelmann, et al., Towards massive connectivity support for scalable mMTC communications in 5G networks, IEEE Access 6 (2018) 28969–28992.

[6] S.T. Chung, A.J. Goldsmith, Degrees of freedom in adaptive modulation: A unified view, IEEE Trans. Commun. 49 (9) (2001) 1561–1571.

[7] R. Rajashekar, K.V.S. Hari, L. Hanzo, Antenna selection in spatial modulation systems, IEEE Commun. Lett. 17 (3) (2013) 521–524.

[8] A. Tom, A. Şahin, H. Arslan, Suppressing alignment: joint PAPR and out-of-band power leakage reduction for OFDM-based systems, IEEE Trans. Commun. 64 (3) (2016) 1100–1109.

[9] D.P. Palomar, J.M. Cioffi, M.A. Lagunas, Joint Tx–Rx beamforming design for multicarrier MIMO channels: A unified framework for convex optimization, IEEE Trans. Signal Process. 5 (9) (2003) 2381–2401.

[10] E. Güvenkaya, H. Arslan, Secure communication in frequency selective channels with fade-avoiding subchannel usage, in: Proc. IEEE Int. Conf. on Commun. Workshops (ICC), 2014, pp. 813–818.

[11] J.M. Hamamreh, H. Arslan, Joint PHY/MAC layer security design using ARQ with MRC and null-space independent PAPR-aware artificial noise in SISO systems, IEEE Trans. Wireless Commun. 17 (9) (2018) 6190–6204.

[12] E. Basar, Ü. Aygölü, E. Panayırcı, H.V. Poor, Orthogonal frequency division multiplexing with index modulation, IEEE Trans. Signal Process. 61 (22) (2013) 5536–5549.

[13] E. Basar, Index modulation techniques for 5G wireless networks, IEEE Commun. Mag. 54 (7) (2016) 168–175.

[14] E. Basar, M. Wen, R. Mesleh, M. Di Renzo, Y. Xiao, H. Haas, Index modulation techniques for next-generation wireless networks, IEEE Access 5 (2017) 16693–16746.

[15] T. Mao, Z. Wang, Q. Wang, S. Chen, L. Hanzo, Dual-mode index modulation aided OFDM, IEEE Access 5 (2017) 50–60.

[16] S. Aldırmaz Çolak, Y. Acar, E. Basar, Adaptive dual-mode OFDM with index modulation, Phys. Commun. 30 (2017) 15–25.

[17] J.M. Hamamreh, E. Basar, H. Arslan, OFDM-subcarrier index selection for enhancing security and reliability of 5G URLLC services, IEEE Access 5 (2017) 25863–25875.

[18] M. Wen, E. Basar, Q. Li, B. Zheng, M, Zhang multiple-mode orthogonal frequency division multiplexing with index modulation, IEEE Trans. Commun. 65 (9) (2017) 3892–3906.

[19] M. Wen, Q. Li, E. Basar, W. Zhang, Generalized multiple-mode OFDM with index modulation, IEEE Trans. Wireless Commun. 17 (10) (2018) 6531–6543.

[20] E. Basar, Multiple-input multiple-output OFDM with index modulation, IEEE Signal Process. Lett. 22 (12) (2015) 2259–2263.

[21] E. Basar, On multiple-input multiple-output OFDM with index modulation for next generation wireless networks, IEEE Trans. Signal Process. 64 (15) (2016) 3868–3878.

[22] S. Doğan, A. Tusha, H. Arslan, OFDM With index modulation for asynchronous mMTC networks, Sensors 18 (4) (2018) 1–15.

[23] E. Basar, OFDM With index modulation using coordinate interleaving, IEEE Wireless Commun. Lett. 4 (4) (2015) 381–384.

[24] Y. Xiao, S. Wang, L. Dan, X. Lei, P. Yang, W. Xiang, OFDM With interleaved subcarrier-index modulation, IEEE Commun. Lett. 18 (8) (2014) 1447–1450.

[25] J. Crawford, E. Chatziantoniou, Y. Ko, On the SEP analysis of OFDM index modulation with hybrid low complexity greedy detection and diversity reception, IEEE Trans. Veh. Technol. 66 (9) (2017) 8103–8118.

[26] T. Van Luong, Y. Ko, A tight bound on BER of MCIK-OFDM with greedy detection and imperfect CSI, IEEE Commun. Lett. 21 (12) (2017) 2594–2597.

[27] E. Chatziantoniou, Y. Ko, Generalized SER analysis of OFDM index modulation for vehicular D2D environments, in: Proc. Int. Conf. Inf. Commun. Technol. Converg. (ICTC), 2018, pp. 436–441.

[28] S. Ahmadi, LTE-Advanced a Practical Systems Approach to Understanding the 3GPP LTE Releases 10 and 11 Radio Access Technologies, Academic, New York, NY, USA, 2014.

Ebubekir Memişoğlu received the B.S. degree in electrical and electronics engineering from Istanbul University, Turkey, in 2016. Currently, he is studying for a Master's degree in telecommunications engineering in Istanbul Technical University, and researcher at the Communications, Signal Processing, and Networking Center, Istanbul Medipol University, Istanbul, Turkey. His current research interests include wireless communications, waveform design, and index modulation.

Ertugrul Basar (S'09-M'13-SM'16) received the B.S. degree (Hons.) from Istanbul University, Turkey, in 2007, and the M.S. and Ph.D. degrees from Istanbul Technical University, Turkey, in 2009 and 2013, respectively. From 2011 to 2012, he was with the Department of Electrical Engineering, Princeton University, Princeton, NJ, USA, as a Visiting Research Collaborator. He is currently an Associate Professor with the Department of Electrical and Electronics Engineering, Koç University, Istanbul, Turkey. Previously, he was an Assistant Professor and an Associate Professor with Istanbul Technical University from 2014 to 2017 and 2017 to 2018, respectively. He is an inventor of four pending/granted patents on index modulation schemes. His primary research interests include MIMO systems, index modulation, cooperative communications, OFDM, visible light communications, and signal processing for communications.

Recent recognition of his research includes the Science Academy (Turkey) Young Scientists (BAGEP) Award in 2018, Turkish Academy of Sciences Outstanding Young Scientist (TUBA-GEBIP) Award in 2017, the first-ever IEEE Turkey Research Encouragement Award in 2017, and the Istanbul Technical University Best Ph.D. Thesis Award in 2014. He is also the recipient of five Best Paper Awards including one from the IEEE International Conference on Communications 2016. He has served as a TPC track chair or a TPC member for several IEEE conferences including GLOBECOM, VTC, PIMRC, and so on.

Dr. Basar currently serves as an Editor of the IEEE Transactions on Communications and Physical Communication (Elsevier), and as an Associate Editor of the IEEE Communications Letters. He served as an Associate Editor for the IEEE Access from 2016 to 2018. He is also the Lead Guest Editor of the IEEE Journal of Selected Topics in Signal Processing October 2019 Special Issue Index Modulation for Future Wireless Networks: A Signal Processing Perspective and Physical Communication January 2019 Special Issue Radio Access Technologies for Beyond 5G Wireless Networks.

Hüseyin Arslan (S'95-M'98-SM'04-F'15) received the B.S. degree from Middle East Technical University, Ankara, Turkey, in 1992, and the M.S. and Ph.D. degrees from Southern Methodist University, Dallas, TX, USA, in 1994 and 1998, respectively. From 1998 to 2002, he was with the Research Group, Ericsson Inc., Charlotte, NC, USA, where he was involved in several projects related to 2G and 3G wireless communication systems. Since 2002, he has been with the Electrical Engineering Department, University of South Florida, Tampa, FL, USA. Since 2014, he has also been the Dean of the College of Engineering and Natural Sciences, Istanbul Medipol University. He was a part-time Consultant for various companies and institutions, including Anritsu Company, Morgan Hill, CA, USA, and the Scientific and Technological Research Council of Turkey. His research interests are in physical layer security, millimeter-wave communications, small cells, multicarrier wireless technologies, coexistence issues on heterogeneous networks, aeronautical (high-altitude platform) communications, in vivo channel modeling, and system design.